

# Determination of power density in VVER-1000 Mock-Up in LR-0 reactor

Michal Košťál \*, Vojtěch Rypar, Davit Harutyunyan, Martin Schulc, Evžen Losa

Research Center Rez Ltd., 250 68 Husinec-Rez 130, Czech Republic

**Abstract.** The pin power density is an important quantity which has to be monitored during the reactor operation, for two main reasons. Firstly, it is part of the limits and conditions of safe operation and, secondly, it is source term in neutron transport calculations used for the adequate assessing of the state of core structures and pressure vessel material. It is often calculated using deterministic codes which may have problems with an adequate definition of boundary conditions in subcritical regions. This may lead to overestimation of real situation, and therefore the validation of the utility codes contributes not only to better fuel utilization, but also to more precise description of radiation situation in structural components of core. Current paper presents methods developed at LR-0 reactor, as well as selected results for pin power density measurement in peripheral regions of VVER-1000 mock-up. The presented data show that the results of a utility diffusion code at core boundary overestimate the measurement. This situation, however satisfactory safe, may lead to unduly conservative approach in the determination of radiation damage of core structures.

## 1 Introduction

The pin power density distribution cannot be measured directly, but it can be determined indirectly via fission density. Such approach is possible due to very low disproportionality between fission and power density. The fission density can be determined by means of gamma spectroscopy of irradiated fuel, where the amount of radioactive fission products and fission density are proportional. This criterion has to be met also in the cases with different spectra, especially near baffle or control rods [1, 2, 3]. Gamma spectroscopy is suitable also for burnup determination [4].

Semiconductor gamma spectrometry with an HPGe coaxial detector in horizontal orientation was used to measure net peak areas (NPA, the area under selected gamma energy peak) of chosen fission products induced in the fuel during its irradiation. Detector is placed in a thick Pb cylindrical shield with various types of collimator. Especially in axial measurement the thin collimator (2×1 cm) has to be used. Measured gamma spectra were analyzed with the Genie 2000 software (Canberra).

## 2 LR-0 reactor

The LR-0 reactor, operated by the Research Centre Rez (the Czech Republic), is a pool type zero power light water reactor. For the layout of the reactor see Figure 1.

All described experiments were performed with the VVER-1000 Mock-Up. This mock-up core consists of 32 shortened VVER-1000 type fuel assemblies with different enrichments of  $^{235}\text{U}$  [3]. The fuel length is optimized for the LR-0 reactor and the fissile column is 125 cm long. The core layout with marked measured fuel pins is shown in Figure 2.

## 3 Experimental and calculation methods

The project, carried out on LR-0 reactor, was focused on fission rates determination in different fuel pins in VVER-1000 Mock-Up core. Positions of selected pins, together with pin numbering, are highlighted on Figure 2. There were carried out 3 irradiation sets to determine the fission density based on both short-living ( $^{92}\text{Sr}$ ,  $^{91}\text{Sr}$ ,  $^{97}\text{Zr}$ ,  $^{135}\text{I}$ ,  $^{88}\text{Kr}$ ; they can be observed immediately after a short irradiation on low power level) and week-living ( $^{140}\text{Ba}$ ,  $^{103}\text{Ru}$ ,  $^{131}\text{I}$ ,  $^{95}\text{Zr}$ ,  $^{140}\text{La}$ ; they can be observed after a long-lasting irradiation on higher power level and after appropriate decay time) fission products. Short living products were measured after 5 irradiation batches on power about 10 W lasting 2.5 hours each. To induce measurable activities of long living products, the fuel was irradiated for 100 hours on power about 700 W. Absolute reactor power was monitored by activation foils. The fission reaction rates measurements were then compared with computational models.

\*Corresponding author: [Michal.Kostal@cvrez.cz](mailto:Michal.Kostal@cvrez.cz)

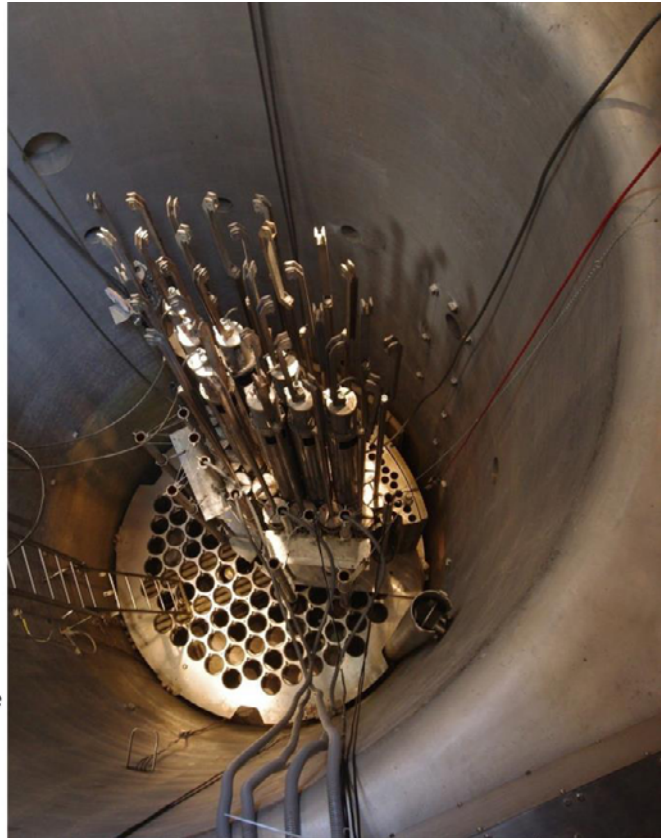
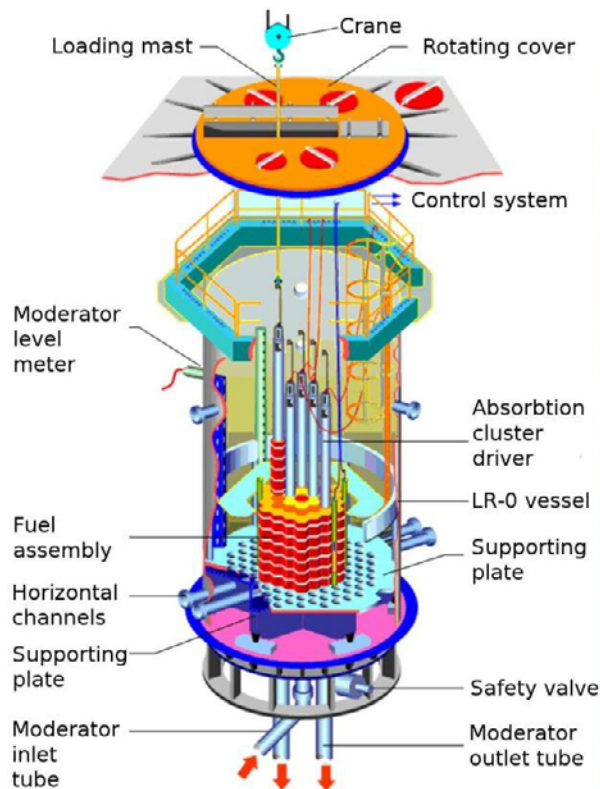


**Figure 1.** General view on LR-0 and Mock-Up core with barrel and baffle simulators

### 3.1. Fission rates measurement

The measurement was performed in the centre of the fissile column. The measured NPA's were corrected to selected reference date. In case of short living fission products, it is the end of irradiation, in other cases selected reference date. That is chosen to the time when all mother nuclides of studied radioisotopes are decayed. In case of  $^{140}\text{La}$  measurement, the reference time is set to transient equilibrium between  $^{140}\text{Ba}$  and  $^{140}\text{La}$ . This correction is applicable only when the photons of the analysed peak, emitted during the decay, occur in the sample [4, 5, 6]. Observed photons can also be extracted in case of mixed peak [7]. This approach of extracting peak of interest from mixed peak was used only in case of  $^{97}\text{Zr}$ .

Net peak areas in different energy peaks of selected fission products induced in the fuel during its irradiation were measured by means of semiconductor gamma spectrometry with an HPGe coaxial detector in a streamline horizontal configuration (Ortec GEM70, resolution approximately 2.1 keV at  $E_\gamma = 1333$  keV). Gamma spectra were measured using multichannel analyser DSA 2000 controlled by computer using Genie 2000 spectroscopy software via the in-built Ethernet interface. Genie 2000 software with gamma analysis package also analysed acquired gamma-spectra.

To suppress the effect of non-homogenous fission products distribution in the fuel, the pins axially rotate during the measurement. This effect could play its role in the pins adjacent to the reactor baffle model and reflects the strong gradient in neutron flux caused by a strong absorption in the steel which forms the reactor baffle model. The theoretical prediction states significant heterogeneities in the distribution of fission products. Namely there are 20% more fission products in the pellet region opposite to the baffle, than in the region near the baffle (see Figure 3) The layout of the experimental arrangement is shown in Figure 4.

#### 3.1.1 Short living fission products

In this experiment, the fission products induced within 2.5 h irradiation on power level  $\sim 10$  W were measured. Under these conditions, the observed fission products have relatively short half-life, thus the pins were measured after 5 irradiation steps. The fuel in this experiment was measured immediately after each irradiation, therefore it was highly radioactive. Due to this fact the dead time for HPGe measurement was very high, thus the signal had to be suppressed by a Pb-Cu plate (3.3 mm of Pb followed by 1 mm of Cu) placed between the measured pin and the HPGe front end cap.

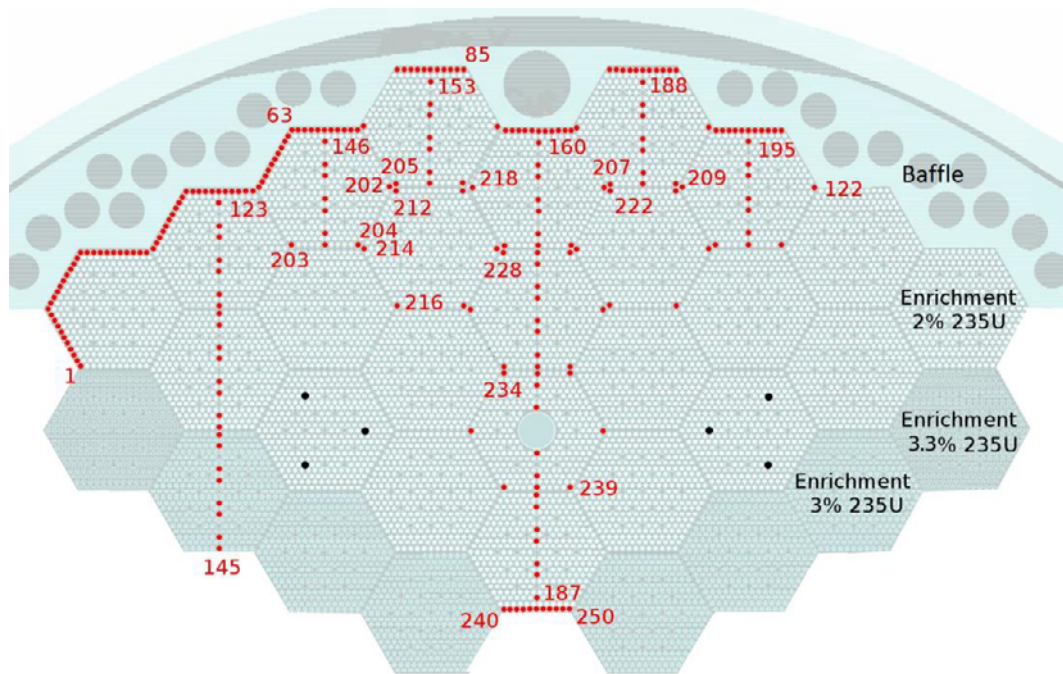


Figure 2. Positions of measured pins

Many peaks can be found in the fuel shortly after the end of irradiation. It reflects high activity of short living fission products after short irradiation. Most notable peaks are presented in Table 1, but it is worth noting that only few of reported fission products are suitable for fission density determination. The comparison between

calculated and measured NPA for selected nuclides is plotted in Figure 5. The satisfactory agreement shows, that not only  $^{92}\text{Sr}$ , but also  $^{91}\text{Sr}$  is suitable for fission density determination. More about this method is presented in [5] and [9].

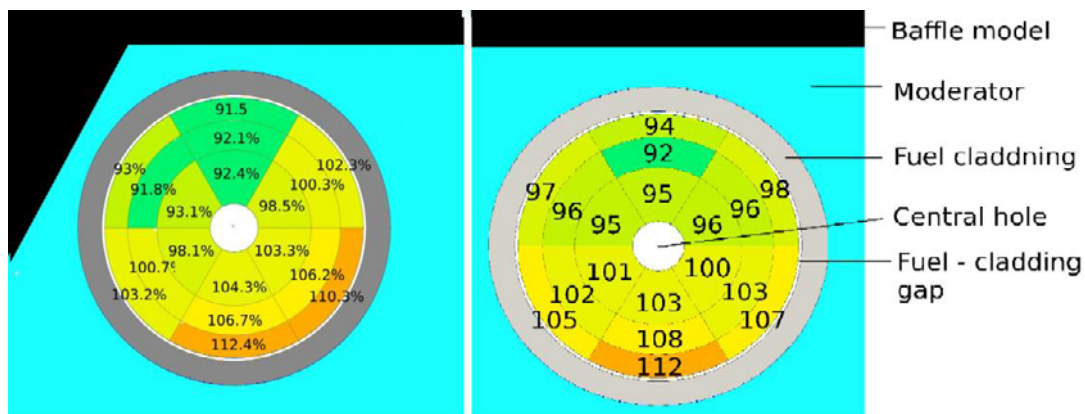


Figure 3. The theoretical prediction of fission distribution in pin near baffle model (% of average fission density)

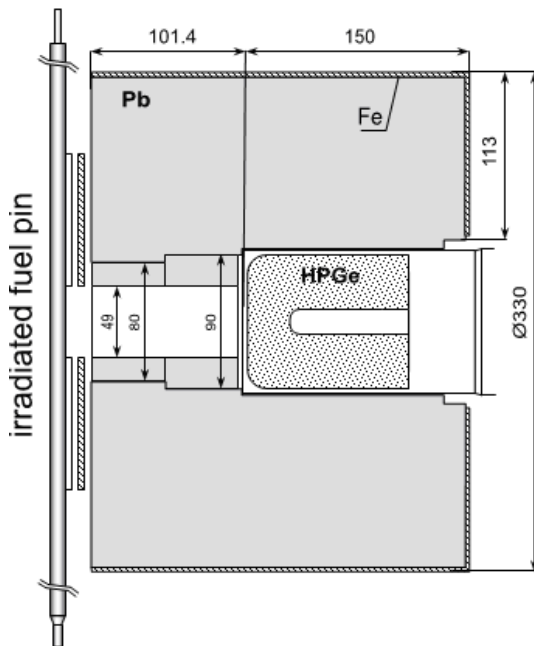
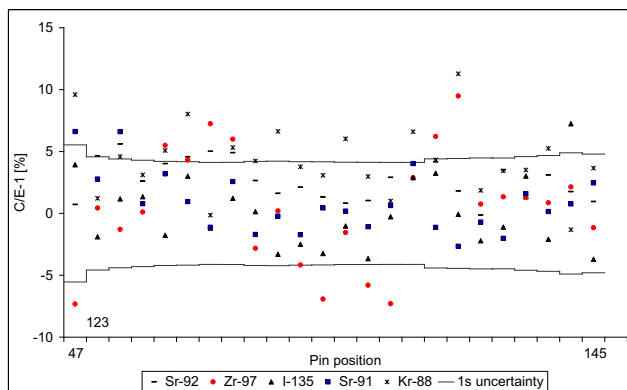
### 3.1.2 Week living fission products

Net peak areas of selected longer-living fission products induced in the fuel during 100 hours irradiation and at least 16 days of decay time were measured. The peaks in the energy interval below 1 MeV were analysed. Specifically these were 537 keV peak for  $^{140}\text{Ba}$ , 498 keV peak for  $^{103}\text{Ru}$ , 365 keV peak for  $^{131}\text{I}$  and 724 keV peak for  $^{95}\text{Zr}$ . The count times were chosen to obtain over  $10^4$  counts in net peak area of  $^{140}\text{Ba}$  peak, thereby achieving

statistical uncertainty less than 1%. The analyzed NPAs varies around  $10^4$ - $10^5$  except measured nuclides  $^{131}\text{I}$  with  $5 \cdot 10^3$  pulses in minimal NPA values. The effect of true summation is neglected, because of the measurement geometry, the low gamma branching ratio of the coincidence peaks, or low energy of the coincidence peaks, as well as low HPGe sensitivity. It was observed good agreement between calculated and measured NPA of studied nuclides. Thus it seems, they are suitable for fission density determination (see Figure 6). The more detailed results of week-living fission products measurement are presented in [6].

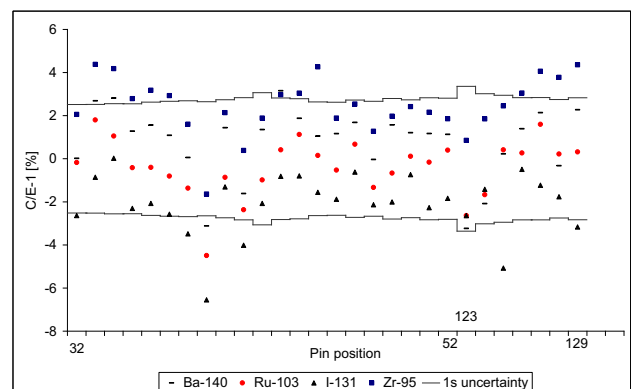
**Table 1.** Radionuclides selected from fuel pin gamma spectra measured 1.2 h after irradiation (irradiation period = 2.5 h, reactor power  $\approx 9.5$  W). Activity values were corrected for radioactive decay to the time of reactor shutdown [1].

| Radioisotope              | Activity (%) | Uncertainty (%) | Key line (keV) | Half-life (h) | Decay scheme  |
|---------------------------|--------------|-----------------|----------------|---------------|---|
| $^{134}\text{I}$          | 100.0        | 1.0             | 847.0          | 0.88          | $^{134}\text{Te} \rightarrow ^{134}\text{I}$          |
| $^{138}\text{Cs}$         | 98.5         | 0.8             | 1435.8         | 0.56          | $^{138}\text{Xe} \rightarrow ^{138}\text{Cs}$         |
| $^{134}\text{Te}$         | 68.2         | 1.1             | 767.2          | 0.70          | $^{134}\text{Te} \rightarrow ^{134}\text{I}$          |
| $^{142}\text{La}$         | 44.1         | 0.9             | 641.3          | 1.52          | $^{142}\text{Ba} \rightarrow ^{142}\text{La}$         |
| $^{133\text{m}}\text{Te}$ | 29.1         | 1.3             | 912.7          | 0.92          | $^{133\text{m}}\text{Te} \rightarrow ^{133}\text{Te}$ |
| $^{92}\text{Sr}$          | 25.1         | 0.8             | 1383.9         | 2.71          | $^{92}\text{Sr} \rightarrow ^{92}\text{Y}$            |
| $^{87}\text{Kr}$          | 19.2         | 3.9             | 402.6          | 1.27          | $^{87}\text{Kr} \rightarrow ^{87}\text{Rb}$           |
| $^{88}\text{Kr}$          | 13.9         | 2.1             | 2392.1         | 2.84          | $^{88}\text{Kr} \rightarrow ^{88}\text{Rb}$           |
| $^{135}\text{I}$          | 13.6         | 1.2             | 1260.4         | 6.57          | $^{135}\text{I} \rightarrow ^{135}\text{Xe}$          |
| $^{91}\text{Sr}$          | 8.5          | 2.0             | 1024.3         | 9.63          | $^{91}\text{Sr} \rightarrow ^{91}\text{Y}$            |
| $^{97}\text{Nb}$          | 8.4          | 2.2             | 657.9          | 1.20          | $^{97}\text{Zr} \rightarrow ^{97}\text{Nb}$           |
| $^{132}\text{Te}$         | 3.5          | 5.9             | 228.2          | 3.2           | $^{132}\text{Te} \rightarrow ^{132}\text{I}$          |
| $^{97}\text{Zr}$          | 5.7          | 2.1             | 743.4          | 16.9          | $^{97}\text{Zr} \rightarrow ^{97}\text{Nb}$           |
| $^{133}\text{I}$          | 4.9          | 2.2             | 529.9          | 20.8          | $^{133}\text{Te} \rightarrow ^{133}\text{I}$          |
| $^{135}\text{Xe}$         | 3.2          | 5.7             | 249.8          | 9.14          | $^{135}\text{I} \rightarrow ^{135}\text{Xe}$          |

**Figure 4.** Vertical layout of power distribution measurement (Dimension are in mm)**Figure 5.** Agreement of NPA measurement with calculation for selected short living fission products.

### 3.1.3. $^{140}\text{La}$ Measurement

The HPGe measurement of pins started 15 days after the reactor shut-down and 1597 keV ( $^{140}\text{La}$ ) energy peak was assessed. Such time is needed for establishing of transient equilibrium between mother  $^{140}\text{Ba}$  and daughter  $^{140}\text{La}$  nuclides. In this transient equilibrium, the decay correction of both radionuclides can be simply calculated by means of the  $^{140}\text{Ba}$  decay half-life (12.75 days). The uncertainties in realized experiment are below 10 %. The power level during irradiation was not defined, that is the reason why the measured data have relative character. Such approach simplifies the evaluation process of experimental data, because otherwise the measured gamma activity of  $^{140}\text{La}$  must be corrected for true summation effect, due to the many coincidence peaks present in its decay scheme.

**Figure 6.** C/E-1 comparison for observed nuclei and ENDF VII calculation

In relative comparison, on the other hand, such correction is not necessary, because all measurements are done in the same geometry and the correction factor is already the same. More details can be found in [6].

### 3.2. Detector arrangement for measurement of activation foils

The value of the mock-up power, which is used for normalization of absolutely measured fission products ( $^{92}\text{Sr}$ ,  $^{91}\text{Sr}$ ,  $^{97}\text{Zr}$ ,  $^{135}\text{I}$ ,  $^{88}\text{Kr}$ ,  $^{140}\text{Ba}$ ,  $^{103}\text{Ru}$ ,  $^{131}\text{I}$ , and  $^{95}\text{Zr}$ ), was determined by means of reaction rate determination in the activation foil using reaction  $^{197}\text{Au}(n,g)^{198}\text{Au}$ . The gold, in mass about 30  $\mu\text{g}$  per foil, was in an aluminium alloy with 1% of Au. The foil diameter was 3.6 mm and its thickness was 0.1 mm. The  $^{198}\text{Au}$  peak at 412 keV was measured immediately after the irradiation by the coaxial HPGe detector in vertical configuration (Ortec GEM35). For background radiation suppression, the detector and measured foil are located in the sandwich shielding box. The experimental uncertainties were estimated to be below 3%. More details can be found in [5].

### 3.3. Calculations

The pin-by-pin fission density distribution in the reactor core was calculated by the MCNP6 [10] transport code in critical mode [11] and ENDF/B-VII.0 library [12].

In case of steel reactor structures and thermal neutron transport, the free gas approach for  $^{56}\text{Fe}$  was used.

The HPGe responses used in evaluation of fission densities of selected fission products were also determined by calculation using the MCNP6 code. The parameters of the detector producer were used for computational model compilation. The yields of the individual nuclides, which contribute to the production of selected isotopes, were used directly from the ENDF/B-VII.0 nuclear data library.

## 4 Results

The fission densities from nuclides induced during defined irradiation were derived using equation (1). The  $^{140}\text{La}$  measurement from 2008 has character of relative distribution of fission rates. The selection of pins for relative measurement contains same 12 pins as selection for absolute measurement, namely pins in position 53, 63 - 73 (see Figure 2). Due to this overlap, the normalization of relative  $^{140}\text{La}$  distribution to fission densities can be realized.

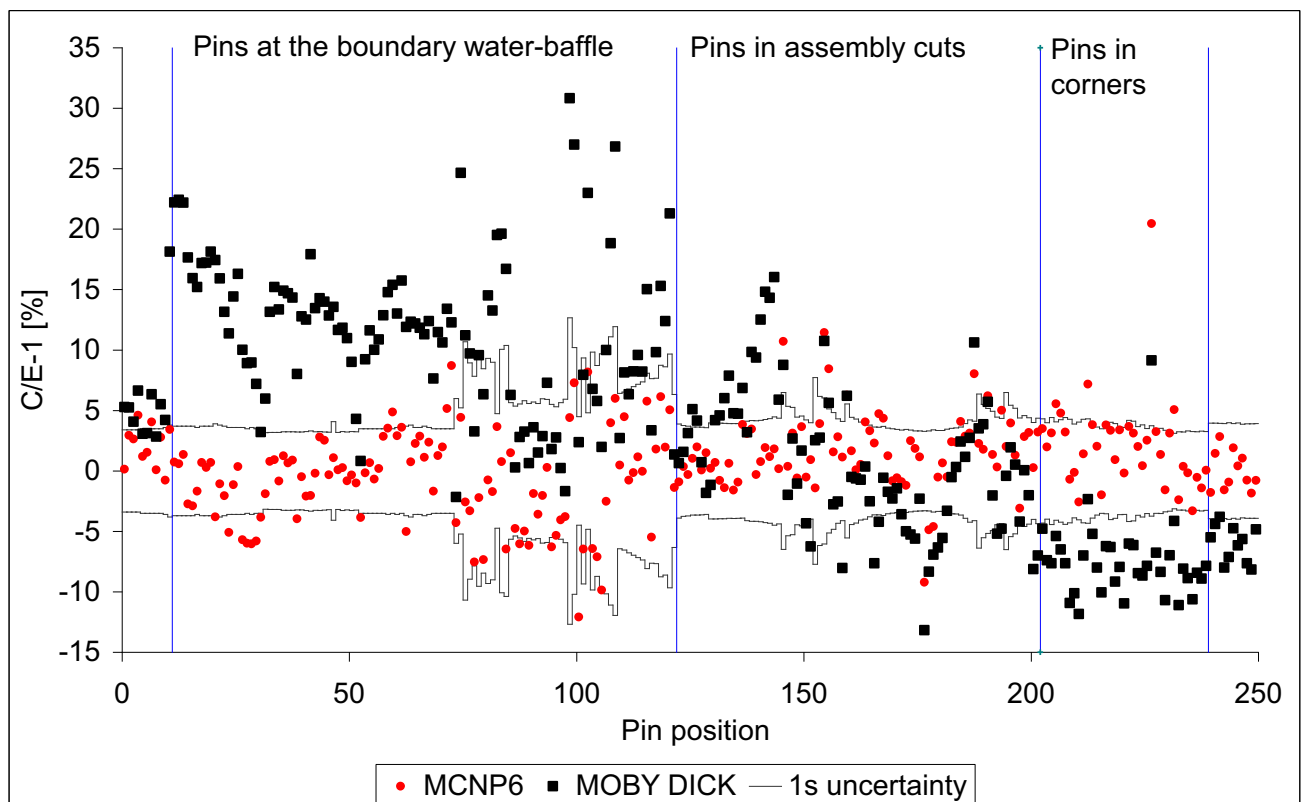


**Figure 7.** Experiment to calculation comparison of fission densities in VVER-1000 Mock-Up by means of C/E-1

$$F_j^i = \frac{NPA_j^i(t)}{\eta^i \cdot \varepsilon^i \cdot \lambda^i} \cdot \frac{1}{N^i(t)} = NPA_j^i(0) \cdot \frac{1}{\eta^i \cdot \varepsilon^i \cdot \lambda^i \cdot N^i(0)} \quad (1)$$

$$NPA_j^i(0) = NPA_j^i(t) \cdot \frac{1}{e^{-\lambda^i \cdot t}} \times \frac{\lambda^i \cdot \Delta T}{1 - e^{-\lambda^i \cdot \Delta T}} \quad (2)$$

$$N^i(0) = \frac{q^i}{\lambda^i} \cdot (1 - e^{-\lambda^i \cdot T_{irr}}) \quad (3)$$

$F_j^i$  fission rate determined via the  $i$ -th nuclei and  $j$ -th pin;  $N^i(t)$  calculated number of observed nuclei in fuel pin when 1 fission/s occurs, in time  $t$  after irradiation end;  $NPA_j^i(t)$  measured Net Peak Area of the observed nuclei and selected peak in  $i$ -th pin (equation (2));  $\lambda^i$  decay constant of selected nuclide;  $\eta^i$  efficiency of HPGe for the selected gamma line of the  $i$ -th nuclide;  $\varepsilon^i$  gamma

branching ratio of the selected peak from observed nuclei  $i$ ;  $t$  start  $i$ -th pin measurement;  $\Delta T$  length of  $i$ -th pin HPGe measurement;  $q^i$  is fission yield of  $i$  th isotope,  $T_{irr}$  is time of irradiation. The resulting fission densities are compared with Monte Carlo MCNP6 and diffusion code MOBY DICK [13] calculations, in form of C/E-1 comparison in, see Figure 7. The comparison covers especially the pins in positions with expected C/E discrepancies, i.e. near the core and baffle boundary, between the assemblies (where water gaps are present) and in the assemblies corners. Especially the diffusion codes may have problems with adequate definition of boundary conditions near the steel internal structures of nuclear reactor. It can be said, that the expectations were fulfilled, and notable discrepancies can be observed in case of diffusion code MOBY DICK results.

Generally, the diffusion code results overestimate experiment in positions near baffle, while in positions in assembly corners they underestimate experiment. It can be explained by the fact, that as steel does not have so good moderation properties as fuel cell (i.e. pin surrounded by water) and the real backscatter from steel is lower than prediction based on parameters derived for fuel cell. In the corners, the situation is opposite; the real moderation properties are better than theoretical prediction for fuel cell, which reflects the overestimation of diffusion calculational approach. Fuel pins of positions on core-stainless steel baffle border have numbering 11–122 and those ones on central axis of fuel assemblies 123–201.

## 5 Conclusions

The methodology, developed at LR-0 reactor, is suitable for experimental determination of fission density. The experimental measurement is in satisfactory agreement with Monte Carlo simulation. In case of diffusion calculation, notable variations in regions in corners and baffle can be observed. Diffusion code MOBY DICK underestimates experiment in corner pins, while near baffle it overestimates. The rate of overestimation can be as high as 25%. It's worth noting, such kind of overestimation is on safe side, because the calculational dose in the RPV overestimates true value. On the other hand the residual lifetime prediction of RPV, based on diffusion code might be unduly conservative.

It can be concluded that fission source described by Monte Carlo code is more reliable than description by diffusion code, therefore it should be used for the serious issues concerning the topics such as RPV lifetime assessment or estimation of the flux behind the reactor vessel.

## Acknowledgements

The presented work was financially supported by the Ministry of Education, Youth and Sport Czech Republic Project LQ1603 (Research for SUSSEN).

## References

1. M. Švadlenková et al., Gamma spectrometry of short living fission products in fuel pins, Nucl. Inst. and Meth. in Physics Research Section A, 739, (2014), pp 55-62,
2. H. Kröhnert et al., Gamma-ray spectrometric measurements of fission rate ratios between fresh and burnt fuel following irradiation in a zero-power reactor, Nucl. Inst. and Meth. in Physics Research Section A, 698, (2013), pp 72-80
3. M. Košťál et al., Effect of inhomogeneities inserted into fuel assembly in the VVER-1000 mock-up on the LR-0 research reactor, Ann. of Nucl. En., 69, (2014), pp 168-174
4. M. Kolečka et al., Determination of IRT-2M fuel burnup by gamma spectrometry, Appl. Rad. and Isot., 107, (2016), pp 92-97
5. M. Košťál et al., Comparison of various hours living fission products for absolute power density determination in VVER-1000 mock up in LR-0 reactor, Appl. Rad. and Isot., 105, (2015), pp 264-272
6. M. Košťál et al., Determination of critical assembly absolute power using post-irradiation activation measurement of week-lived fission products, Appl. Rad. and Isot., 89, (2014), pp 18-24
7. M. Košťál, V. Rypar, M. Švadlenková, The pin power distribution in the VVER-1000 mock-up on the LR-0 research reactor, Nucl. Eng. and Des., 242, (2012), pp 201-214
8. M. Košťál, M. Švadlenková, J. Milčák, The application and comparison of  $^{97}\text{Zr}$  and  $^{92}\text{Sr}$  in the absolute determination of the contribution of power density and cladding activation in a VVER-1000 Mock-Up on the LR-0 Research Reactor, Nucl. Inst. and Meth. in Physics Research Section A, 738, (2014), pp 87-92
9. U.C. Bergmann et al, Optimised non-invasive method to determine  $^{238}\text{U}$ -captures-to-total-fissions in reactor fuel, Nucl. Inst. and Meth. in Physics Research Section A, 556, 1, (2006), pp 331-338
10. D.B. Pelowitz (Ed.), MCNP6™ User's Manual, Los Alamos National Laboratory Report, LA-CP-13-00634 (2013)
11. T. Goorley, et al., "Initial MCNP6 Release Overview", Nuclear Technology, 180, pp 298-315 (Dec 2012).
12. M.B. Chadwick et al, ENDF/B-VII.0: Next Generation Evaluated Nuclear Data Library for Nuclear Science and Technology, Nuclear Data Sheets, 107, 12, (2006), pp 2931-3060
13. C. Guler, S. Levine, K. Ivanov et al, Development of the VVER core loading optimization system, Ann. of Nucl. En., 31, 7, (2004), pp 747-772